

# Modeling and testing of a silica gel packed-bed system

JUNG-YANG SAN† and GWO-DONQ JIANG

Department of Mechanical Engineering, National Chung-Hsing University, 250, Kuo-Kuang Road, Taichung, Taiwan, R.O.C.

(Received 28 April 1993 and in final form 12 November 1993)

**Abstract**—A two-column packed-bed desiccant dehumidification system is tested and analytically modeled. The results are consistent. The desiccant is a spherical silica gel particle with an average diameter of 5 mm. The length of the columns are individually 9, 15 and 24 cm. Three regeneration temperatures are used, namely, 65, 75 and 85°C. An optimum operating time period is obtained. The heat and mass transfer is analyzed by using a solid-side resistance method with consideration of a fluid friction effect. The magnitude of the fluid friction effect is governed by the Reynolds number and a nondimensional length factor. For a long column or a high inlet air velocity the fluid friction effect becomes significant.

## 1. INTRODUCTION

PACKED-BED systems can be used in adsorption of water vapor, organic solvent and some toxic gases. For a specific adsorbed substance an adequate adsorbent needs to be selected. For example, active carbon is usually used for adsorption of oil or organic solvent. Silica gel and molecular sieves are used for adsorption of water vapor.

A packed-bed system usually consists of two columns which are filled with an adsorbent (Fig. 1). The two columns are arranged in a periodic-switched operation. While one is for adsorption, the other is for desorption. In order to proceed a cyclic operation, an input heat is required for the regeneration of the adsorbent in the desorption process. The amount of the input heat is usually indicated by the temperature of the air for regeneration. Thus the regeneration temperature is a factor affecting the system performance. Besides the regeneration temperature, type of desiccant material, air mass flowrates, cyclic switching period, column length and cross-sectional area, inlet air temperature and humidity ratio are the other factors governing the performance of a packed bed.

Pesaran and Mills [1, 2] studied the moisture transport in a packed-bed system with particular attention to solid-side resistance to moisture difference in the adsorbent particles. Part I of their work is a report of an analytical study of the transient response of a thin silica gel packed bed to a step change in inlet air humidity and temperature. In part II an experimental program which verified the analytical model was conducted. The study only considered the dynamic response of a simple adsorption process and the cyclic operation of the packed-bed system was not investigated.

A comparison between the result of experimental measurement and that of theoretical analysis for a thin silica gel packed bed was performed by Clark *et al.* [3]. The analysis was based on a gas-side controlled heat and mass transfer model which incorporates the solid-side diffusion resistance in a gas-side mass transfer coefficient. In the comparison a high predicted initial rate of adsorption was obtained. The sorption rate and apparent solid-side diffusivity of water in silica gel was studied by Kruckels [4] and Lu *et al.* [5]. In both works the surface diffusion is verified to be the most important mechanism for water vapor adsorbed by regular density silica gel. Thus the ordinary diffusion and Knudsen diffusion can be neglected in theoretical analysis.

Packed-bed systems can be applied to many industrial drying processes, such as the dehumidification of plastic beads in precise injection molding processes, agricultural or industrial warehouse humidity control and the dehumidification of high pressure air supplied

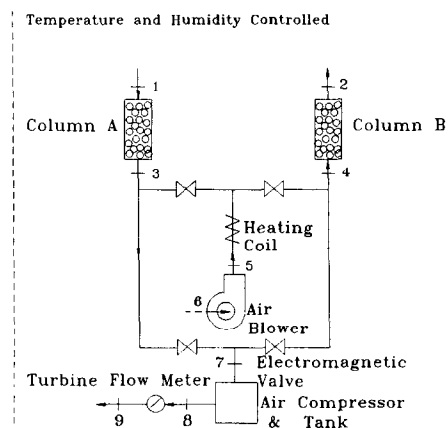


FIG. 1. Schematic of a packed-bed system.

†Author to whom all the correspondence should be sent.

## NOMENCLATURE

1-9	measuring points	$t^*$	nondimensional time, $t/\tau$
$A$	cross-sectional area of column [m <sup>2</sup> ]	$T, T_a$	temperature [°C or K]
$A_c$	column free flow area [m <sup>2</sup> ]	$T^*$	nondimensional temperature, $T/T_{in}$
$A_s$	column total heat or mass transfer area [m <sup>2</sup> ]	$V$	inlet air velocity [m s <sup>-1</sup> ]
$Bi_m$	mass transfer Biot number, $K_G R / \rho_p D_{s,eff}$	$w$	moisture content [kg H <sub>2</sub> O (kg dry desiccant) <sup>-1</sup> ]
$c$	specific heat [kJ kg <sup>-1</sup> K <sup>-1</sup> ]	$Y, \Delta Y$	humidity ratio or humidity removal [kg H <sub>2</sub> O (kg dry air) <sup>-1</sup> ]
$c_{p,e}$	constant pressure specific heat of humid air [kJ kg <sup>-1</sup> K <sup>-1</sup> ]	$z$	axial coordinate [m]
$c_{p,l}$	constant pressure specific heat of water vapor [kJ kg <sup>-1</sup> K <sup>-1</sup> ]	$z^*$	nondimensional axial coordinate, $z/L$
$d$	diameter of column [m]	Greek symbols	
$C^*$	mass ratio of silica gel to processed air in adsorption, $\rho_b AL / \dot{m}_G \tau$	$\gamma$	ratio of air mass flowrates (adsorption/desorption)
$D^*$	nondimensional surface mass diffusion parameter, $D_{s,eff} \tau / R^2$	$\gamma_1$	$H_{ads} / c_b$
$D_{s,eff}$	effective surface mass diffusion coefficient [m <sup>2</sup> s <sup>-1</sup> ]	$\gamma_2$	$c_{p,e} / c_b$
$f$	fluid friction coefficient	$\gamma_3$	$c_{p,l} / c_{p,e}$
$G_a$	air mass flux, $\dot{m}_G / A$ [kg m <sup>2</sup> s <sup>-1</sup> ]	$\varepsilon$	porosity
$h$	enthalpy [kJ kg <sup>-1</sup> ]	$\theta$	fraction of time in a mode [s]
$h_c$	convective heat transfer coefficient [W m <sup>-2</sup> K <sup>-1</sup> ]	$\nu$	kinematic viscosity [m <sup>2</sup> s <sup>-1</sup> ]
$H_{ads}$	heat of adsorption [kJ (kg H <sub>2</sub> O) <sup>-1</sup> ]	$\rho$	density [kg m <sup>-3</sup> ]
$K_G$	gas-side mass transfer coefficient [kg m <sup>-2</sup> s <sup>-1</sup> ]	$\sigma$	nondimensional length factor, see equation (4)
$L$	column length [m]	$\tau$	half-cycle period [min]
$Le$	overall Lewis number, $h_c / K_G c_{p,e}$	$\phi$	relative humidity [%]
$m_1$	mass fraction of water vapor in humid air [kg H <sub>2</sub> O (kg humid air) <sup>-1</sup> ]	Subscripts	
$\dot{m}_G$	mass flowrate of humid air in adsorption [kg s <sup>-1</sup> ]	0	initial value
$n$	water vapor mass flux [kg m <sup>-2</sup> s <sup>-1</sup> ]	1	water vapor
$Ntu$	number of mass transfer units, $K_G \rho L / \dot{m}_G$	ads	adsorption
$P$	pressure [mm Hg or atm]	ave	average value
$\Delta P$	pressure drop [mm Hg or atm]	b	packed bed
$p$	perimeter of column, $A_s / L$ [m]	e	humid air in the stream
$r$	radial coordinate [m]	G	regeneration
$r^*$	nondimensional radial coordinate $r/R$	in	inlet
$R$	particle radius [m]	m	average value
$Re$	Reynolds number, $2RV/\nu$	max	maximum value
$t$	time [s]	opt	optimum value
		out	outlet
		p	particle
		s	surface
		sat	saturation
		total	humid air pressure.

from air compressors, etc. Although a packed-bed system has a higher pressure drop than the newly developed honey-comb type rotary wheel system, its low first cost and low maintenance cost are still attractive to some specific applications.

In this work a transient response of a packed-bed system in a periodic steady-state operation is investigated. The used adsorbent is a regular density silica gel particle. The variation of temperature and humidity in the air streams is measured and the result

is compared to that of a computer analysis with a solid-side diffusion resistance model. In the work the factors dominating the fluid friction effect are discussed. It is also intended to obtain the amount of dehumidification of the system for various operating conditions.

## 2. MATHEMATICAL MODEL

The transient response of the heat and mass transfer in many thin packed beds was analyzed by using the

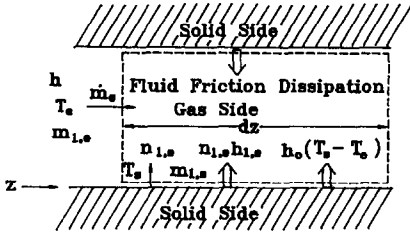


FIG. 2. Heat and mass transfer in a pseudo-channel.

pseudo-gas-side controlled model (PGC) [1]. In the model the overall mass transfer from the air stream to the adsorbent is represented by a gas-side coefficient which is reduced to account for solid-side resistance. Recently, Pesaran and Mills [1] proposed a solid-side resistance model (SSR) for predicting the transient response of the heat and mass transfer in thin silica gel packed beds. The model includes both solid and gas-side resistances in the analysis of the diffusion of water vapor. Thus it is more delicate and accurate than the PGC model. In this work the solid-side resistance model is modified by adding a fluid friction effect. The fluid friction effect may play an important role in a long column packed bed or in the operation with a high air mass flowrate.

In the solid-side resistance model [1] the equilibrium condition on the surface of the silica gel particle is initially evaluated. The result then provides the information in the analysis of the heat and mass transfer in the pseudo-channels of the column (Fig. 2). In this work, a published isotherm equation [1, 6] for a regular density silica gel is used and a corresponding expression of the heat of adsorption is adopted [1, 6]. Based on the above assumptions and using several defined nondimensional variables and parameters, the governing equations can be rearranged in the following forms [1, 6]: (i) Mass diffusion in the particle:

$$\frac{\partial w}{\partial t^*} = \frac{1}{r^{*2}} \frac{\partial}{\partial r^*} \left( r^{*2} D^* \frac{\partial w}{\partial r^*} \right) \quad (1)$$

initial condition:  $w(r^*, z^*, t^* = 0) = w_0(r^*, z^*)$

boundary conditions:  $\left. \frac{\partial w}{\partial r^*} \right|_{r^*=0} = 0$

$$\left. \frac{\partial w}{\partial r^*} \right|_{r^*=1} = -Bi_m(m_{1,s} - m_{1,e})$$

(ii) Equilibrium relationship [1, 6]:

$$m_{1,s} = \frac{0.622\phi_s \cdot P_{\text{sat}}(T_s)}{P_{\text{total}} - 0.378\phi_s \cdot P_{\text{sat}}(T_s)} \quad (2)$$

where

$$\phi_s = 0.0078 - 0.05759w_s + 24.1655w_s^2 - 124.478w_s^3 + 204.226w_s^4$$

(iii) Mass transfer of water vapor in the air stream:

$$\frac{\partial m_{1,e}}{\partial z^*} = Ntu(m_{1,s} - m_{1,e})(1 - m_{1,e}) \quad (3)$$

(iv) Energy balance in the air stream:

$$\begin{aligned} \frac{\partial T_e^*}{\partial z^*} = Ntu[Le(T_s^* - T_e^*) + \gamma_1(T_s^* - T_e^*)(m_{1,s} - m_{1,e})] \\ + \left( \frac{1}{2c_{p,e}T_{in}} \right) \left( \frac{G_a}{\rho_m \epsilon_b} \right)^2 \cdot f \cdot (A_s/A_c) \quad (4) \end{aligned}$$

boundary condition:  $T_e^*(z^* = 0, t^*) = 1.0$

where

$$f[7-9] = \begin{cases} 19.336 Re^{-0.616}, & 0 \leq Re < 200 \\ 4.064 Re^{-0.313}, & 200 \leq Re < 500 \\ 1.478 Re^{-0.15}, & 500 \leq Re < 5000 \end{cases}$$

$$\begin{aligned} \left( \frac{1}{2c_{p,e}T_{in}} \right) \left( \frac{G_a}{\rho_m \epsilon_b} \right)^2 f \cdot (A_s/A_c) \\ = \left[ \frac{3v^2 \cdot L(1 - \epsilon_b)}{8c_{p,e}T_{in}R^3 \cdot \epsilon_b^3} \right] (f Re^2) \equiv \sigma(f Re^2) \end{aligned}$$

(v) Energy balance in the solid:

$$\frac{\partial T_s^*}{\partial t^*} = \frac{Ntu}{C^*} [Le \cdot \gamma_2(T_e^* - T_s^*) + \gamma_3(m_{1,s} - m_{1,e})] \quad (5)$$

initial condition:  $T_s^*(z^*, t^* = 0) = T_0/T_{in}$ .

In the above governing equations  $Ntu$  is the number of transfer units of mass transfer. Similar to that of heat transfer, its value is proportional to moisture transfer coefficient, column length, column perimeter and inversely proportional to air mass flowrate.  $Bi_m$  is the Biot number of mass diffusion in the particle. Its value increases with the gas-side mass transfer coefficient,  $K_G$  [1] and decreases with the effective solid-side surface mass diffusion coefficient,  $D_{s,\text{eff}} \cdot C^*$  can be analogous to the capacity rate ratio in heat exchanger theory. If so,  $(\rho_b AL/\tau)$  will be viewed as the column capacity rate and  $\dot{m}_G$  will be the flow-stream capacity rate. The last term in equation (4) attributes to the fluid friction effect in the column. A specific expression of  $f$  is adopted [7-9] and for the convenience of application the result is recurvefitted in the above form. As shown in equation (4)  $f$  is proportional to a power of Reynolds number and the power varies from  $-0.616$  to  $-0.15$ . Thus the fluid friction effect is proportional to the Reynolds number to the power from 1.384 to 1.85. Besides the Reynolds number the fluid friction effect is also linearly proportional to a nondimensional length factor,  $\sigma$ . In this work the particle radius and inlet air temperature are fixed. Thus an increase of the value of  $\sigma$  directly means an increase of the column length.

Equations (1)–(5) are the governing equations for the heat and mass transfer. The five unknowns are  $w$ ,  $m_{1,s}$ ,  $m_{1,e}$ ,  $T_e^*$  and  $T_s^*$ . Equation (1) is solved using a Crank–Nicholson scheme and the rest equations are solved using a fourth-order Runge–Kutta scheme.

The values of  $c_b$  and  $w_{ave}$  are integrated using a composite Simpson's scheme. In the analysis the value of  $w_{ave}$  is used to evaluate the heat of adsorption and  $c_b$ .

### 3. EXPERIMENTAL APPARATUS AND PROCEDURE

In the experiment, the length of the columns are individually 9, 15 and 24 cm. The inner diameter of the column is 5 cm. The air on the regeneration side is supplied by a one-horsepower centrifugal blower which provides the system with an air volumetric flowrate of  $6.6 \times 10^{-3} \text{ m}^3 \text{ s}^{-1}$  (Fig. 1). The air on the adsorption side is sucked by a two-horsepower reciprocating compressor which can be regulated to result in a variable air mass flowrate. The cyclic switch of the air is controlled by four electromagnetic valves with an inner diameter of 2 in. On the regeneration side the air is heated by an electric heating coil with a maximum output power of 1000 W. The heated air temperature is set up at 65, 75 and 85°C, respectively by adjusting an on-off temperature controller. A programmable controller is used to set up the timing to turn on or off electromagnetic valves. Thus the cyclic switch can be accurately executed.

In the work the inlet air for the adsorption and desorption is directly extracted from the test room. The air temperature and humidity ratio in the room is separately controlled by a heater and a humidifier. A solid plate is placed between the two columns to prevent the exhaust regenerative air being sucked into the adsorption stream. Besides that, a fan slowly blows the air to the system in order to achieve a good recirculation.

The relative humidities are measured by using five thin film capacitance type hygrometers (I-100, Rotronic Co.). The conversion of relative humidity to humidity ratio is performed by using an ASHRAE equation [10]. One of the five hygrometers is used to measure the room temperature and humidity; the other four are individually installed at points 1, 2, 6, 9 in Fig 1. The hygrometers have a response time constant of 10 s and they are calibrated at a suitable temperature and relative humidity to ensure a 5% error of the humidity ratio in the range of measurement. Several T-type thermocouples are used to capture the transient response of the air temperature. The diameter of the T-type thermocouples is 0.1 mm and the response time constant is measured to be less than 6 s. The error of the thermocouples in the temperature measurement is  $\pm 0.5^\circ\text{C}$ . The air volumetric flowrates are measured by using a calibrated floating-ball tube and a turbine flowmeter (EG & G Co.). The uncertainty of the former is 5% and the latter is within 2%. The static pressure drops are measured by using a U-tube filled with mercury and a less than 5% error is assured. In the experiment a pressure drop range from 100 to 106 mm Hg on the desorption side and from 10 to 57 mm Hg on the adsorption side is measured. The transient response of the temperature and relative humidity are automatically recorded by a HP-3852

data acquisition system which assures a cyclic recording time period less than 5.5 s.

In this experiment dyed silica gel particles with diameters of 5 mm are used. The silica gel particles have a density of  $1008 \text{ kg m}^{-3}$  which is classified as a regular density silica gel. During the process of adsorption the color of the particles will change from blue to pink. Thus a good observation of the water vapor adsorption in the transparent column is achieved. However, for the sake of compactness it is not shown in this paper.

In summary, the characteristic factors affecting the performance of the packed-bed system are: (i) regeneration temperature, (ii) cyclic operating time period, (iii) air mass flowrate ratio and inlet air velocity, (iv) column length to diameter ratio, (v) inlet air humidity, (vi) inlet air temperature, (vii) characteristics of silica gel. In this work items (i)–(v) in the above list are individually varied. The other factors are kept the same in the measurement. Thus the time period setting in the PLC, temperature controller of the heating coil, inlet air humidity and air mass flowrate for adsorption are required to be adjusted. The length to diameter ratio is varied by replacing the two columns with different lengths.

### 4. RESULTS

In Fig. 3 the variation of the exit air temperature and humidity ratio in the adsorption/desorption stream is shown. The first point in the adsorption stream actually corresponds to the remaining air in the column during the switch from desorption to adsorption. Thus the temperature and humidity ratio are relatively high. As the process proceeds, the bed temperature starts to descend and the temperature and humidity ratio of the processed air are much lower than those of the initial remaining air in the column. Thus the exit air temperature and humidity ratio tend to descend. However, as more water vapor is adsorbed

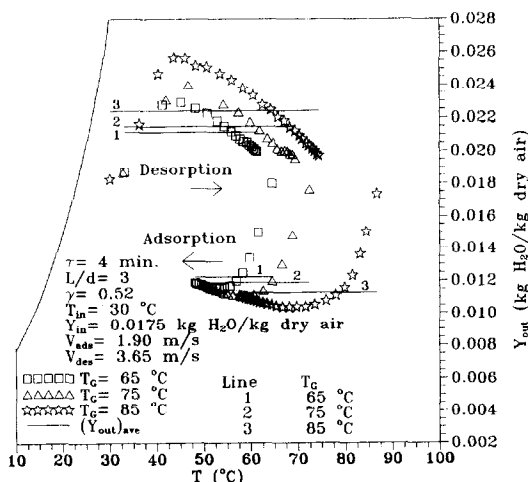


Fig. 3. Air temperature and humidity ratio in an adsorption/desorption stream.

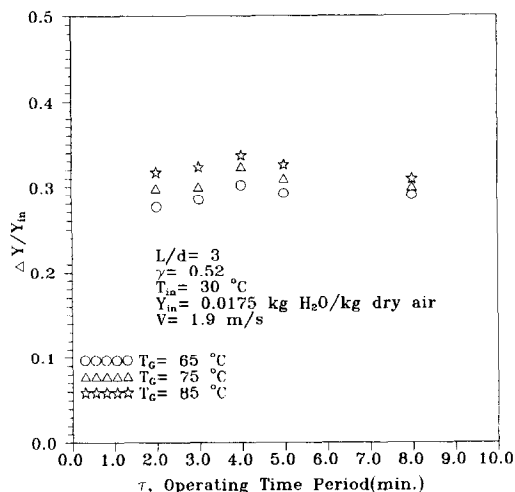


FIG. 4. Dependency of humidity removal on adsorption time and regeneration temperature.

by the desiccant, the dehumidification ability of the desiccant would be degraded. Eventually the humidity ratio of the exit air will rise. Figure 3 also shows the variation of the exit air temperature and humidity ratio in the desorption stream. On the contrary the remaining air in the column during the switch from adsorption to desorption results in a low initial exit air temperature and humidity ratio. As the process proceeds, more moisture comes off the desiccant. The humidity ratio of the regenerative air at the exit increases until it reaches a maximum. Passing the maximum, the desiccant is relatively dry and less water vapor is desorbed. Thus the humidity ratio of the regenerative air will descend.

Figure 4 shows the average humidity removal for various regeneration temperatures and operating time periods. In the diagram the operating time period,  $\tau$ , corresponds to the time period for adsorption. In this work the adsorption time period is the same as the desorption time period. Thus the value of  $\tau$  is actually a half of the cycle time. Figure 4 indicates that either a long or a short time period will degrade the dehumidification ability of the system. Thus an optimum time period exists for each regeneration temperature. From the result it shows that the optimum operating time period is much less than the required time period for water diffusing from the particle surface to the center. Thus very soon the surface of the particle becomes inactive for adsorption. This also implies that most of the interior volume of the particle is ineffective for the process. The above problem can be solved by reducing the air velocity. A reduction of the air velocity may reduce the adsorption rate on the surface of the particle. This provides the particle with sufficient time to diffuse the water from the surface to the interior. Thus the surface is kept active in the process and the humidity removal can be upgraded. The result also shows that the higher the regeneration temperature the higher the value of the average

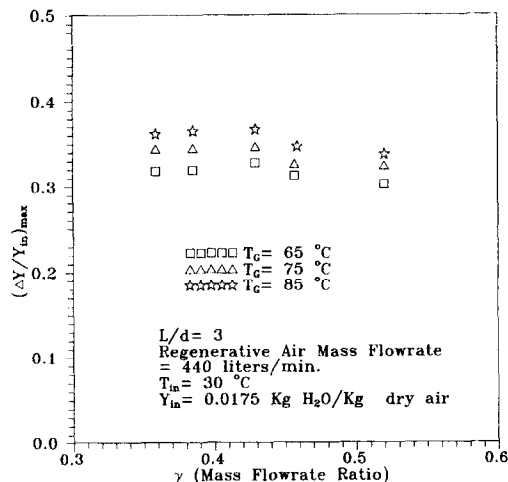


FIG. 5. Humidity removal for various adsorption air mass flowrate.

humidity removal. A higher regeneration temperature may bring the silica gel particles to a drier condition. Thus it can upgrade the system performance. On the other hand, a higher regeneration temperature also may bring the packed bed to a higher temperature. This will deteriorate its performance in adsorption. Thus the humidity removal is not proportional to the regeneration temperature. However, for a higher regeneration temperature the required air mass flowrate on the desorption side can be reduced.

Figure 5 indicates the humidity removal for various adsorption air mass flowrate. Every point in Fig. 5 corresponds to a similar maximum point in Fig. 4. The result shows that an optimum air mass flowrate exists for every regeneration temperature. As the adsorption air mass flowrate increases the maximum humidity removal drops dramatically.

Figure 6 shows the effect of the inlet air humidity on the humidity removal. The result indicates that the system has a high humidity removal for a low humidity operation. The adsorption characteristics of

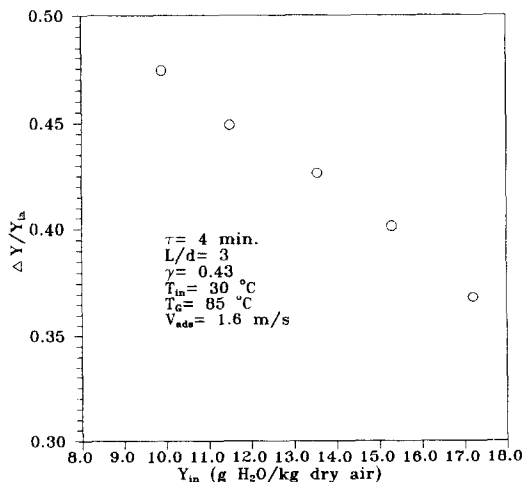


FIG. 6. Effect of inlet air humidity on humidity removal.

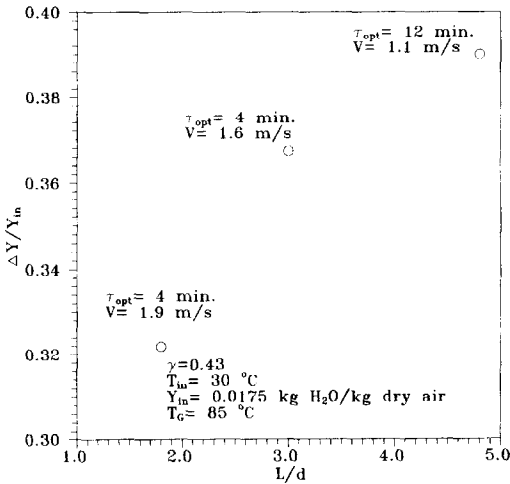


FIG. 7. Effect of column length.

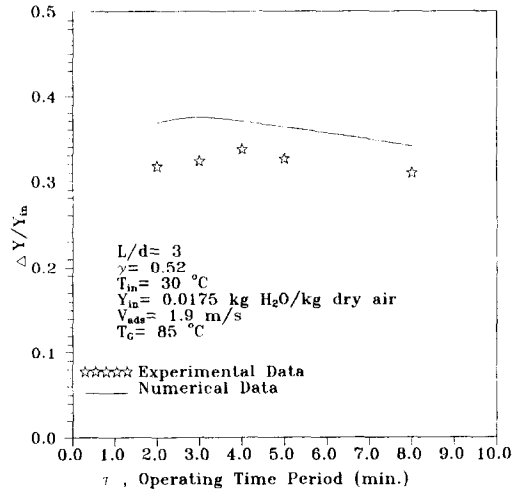


FIG. 9. Comparison of humidity removal for various operating time periods.

the silica gel particles depends on the slope of the isotherms. In the low humidity region the slope is much steeper than that in the high humidity region. Thus the system tends to have a better humidity removal. Besides that, a lower inlet humidity results in a low silica gel moisture content. This in turn will increase the solid-side diffusivity and system uptake. Although the result in Fig. 6 is based on a specific operating condition, it is believed to be a general trend for silica gel adsorption.

Figure 7 shows the effect of column length on the humidity removal. The  $N_{tu}$  is proportional to the column length and inversely proportional to the inlet air velocity. Thus the result also indicates the effect of the  $N_{tu}$  on the system performance. As shown in the diagram a longer column results in a higher humidity removal. However, due to a higher pressure drop the air mass flowrate will be reduced. A longer column containing more silica gel will process a smaller amount of the humid air, thus the optimum operating time period is increased.

Figure 8 represents a comparison between the measured data and analytical result. Since the operation is with a moderate column length and air velocity, the analytical result is obtained without consideration of the fluid friction effect. As can be seen the computer modeling provides an acceptable agreement with the experimental data. The minor discrepancy might be due to the inaccuracy in the measurement and the selected expression of the isotherm and heat of adsorption. Figure 9 represents a comparison of the humidity removal between the measured data and analytical result. As shown in the diagram the predicted humidity removal is higher than the measured data.

Figure 10 shows the prediction of the heat and mass transfer in the packed bed with/without consideration of the fluid friction effect. It is found that the fluid friction effect plays an important role in the case with a high Reynolds number or a long column. As can be observed from Fig. 10 for the case with the Reynolds number of 500,  $\sigma$  of  $2.77 \times 10^{-8}$ ,  $C^*$  of 0.2 and  $N_{tu}$  of

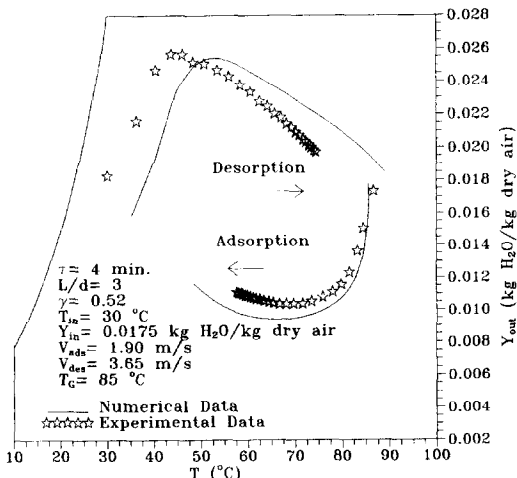


FIG. 8. Comparison of the data on the adsorption/desorption side.

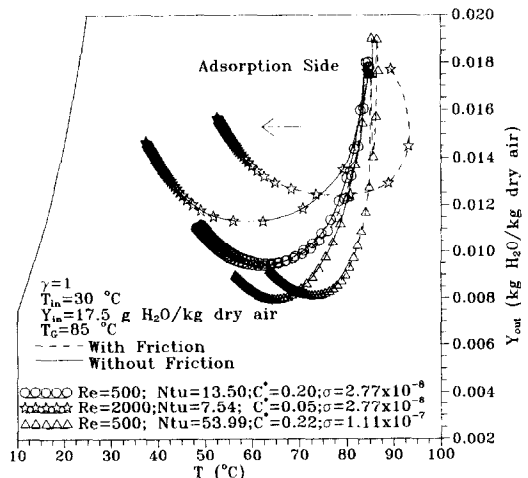


FIG. 10. Predictions with/without consideration of the fluid friction effect.

13.5, the difference between with and without fluid friction is very minor. However, as the value of  $\sigma$  or Reynolds number increases, the discrepancy between the two analyses is enlarged. The result also shows that the effect of the Reynolds number on the fluid friction effect is more important than that of the  $\sigma$ . This phenomenon can be explained by the pressure drop term in the energy equation for the fluid. As mentioned earlier, the fluid friction effect is proportional to the Reynolds number to the power from 1.384 to 1.85 and it is only linearly proportional to the  $\sigma$ .

## 5. CONCLUSIONS

A simulation model for the heat and mass transfer in the silica gel packed-bed system with the consideration of the fluid friction effect is developed. The result is consistent with the measured data. The fluid friction effect is related to the Reynolds number and column length. For the operation with a high Reynolds number or a long column the fluid friction effect becomes crucial. Without considering the fluid friction effect the predicted value of the humidity removal might be overestimated.

The packed-bed system is a device for the dehumidification of humid air without following the traditional dew-point principle. In the experiment the inlet air velocity of the column is relatively high, thus the measured value of the humidity removal is low. However, the general trend of the humidity removal is obtained from the results. The higher the regeneration temperature, the higher the humidity removal. An optimum cycle time is obtained for the system with a specific regeneration temperature and air mass flowrate ratio. The optimum cycle time corresponds to the operation with a maximum humidity removal. The higher the regeneration temperature, the shorter the optimum cycle time. But the variation of the optimum cycle time is very minor.

For the considered range of regeneration tem-

perature an optimum air mass flowrate ratio is found. The optimum air mass flowrate ratio is very less dependent on the regeneration temperature. The column length is also an important factor affecting the humidity removal. An increase of the column length will result in an increase of the system uptake. However, the pressure drop and heat dissipation will tend to increase. The inlet air humidity ratio has a strong influence on the humidity removal. For the considered conditions the humidity removal linearly increases with a decrease of the inlet air humidity ratio.

## REFERENCES

1. A. A. Pesaran and A. F. Mills, Moisture transport in silica gel packed beds—I. Theoretical study, *Int. J. Heat Mass Transfer* **30**, 1037–1049 (1987).
2. A. A. Pesaran and A. F. Mills, Moisture transport in silica gel packed beds—II. Experimental study, *Int. J. Heat Mass Transfer* **30**, 1051–1060 (1987).
3. J. E. Clark, A. F. Mills and H. Buckberg, Design and testing of thin adiabatic desiccant beds for solar air conditioning applications, *J. Solar Energy Engng* **103**, 89–91 (1981).
4. W. W. Kruckels, On gradient dependent diffusivity, *Chem. Engng Sci.* **28**, 1565–1576 (1973).
5. L. T. Lu, D. Charoensupaya and Z. Lavan, Determination of sorption rate and apparent solid-side diffusivity of pure H<sub>2</sub>O in silica gel using a constant volume variable pressure apparatus, *J. Solar Energy Engng* **113**, 257–263 (1991).
6. A. A. Pesaran, Moisture transport in silica gel packed beds, Ph.D. Dissertation, School of Engineering and Applied Sciences, University of California, Los Angeles (1983).
7. J. E. Coppage and A. L. London, Heat transfer and flow friction characteristics of porous media, *Chem. Engng Prog.* **52**, 57–67 (1956).
8. W. M. Kays and A. L. London, *Compact Heat Exchanger*. McGraw-Hill, New York (1984).
9. W. H. Denton, C. H. Robinson and R. S. Tibbs, The heat transfer and pressure loss in fluid flow through randomly packed spheres, HPC-35, US AEC Tech. Information Div., Oak Ridge, Tenn. (1949).
10. *ASHRAE Handbook of Fundamentals*. American Society of Heating, Refrigeration and Air-Conditioning Engineers (1981).